A Cluster-based Analysis of Outdoor-to-Indoor Office MIMO Measurements at 5.2 GHz

Shurjeel Wyne[1], Nicolai Czink[2], Johan Karedal[1], Peter Almers[1], Fredrik Tufvesson[1], and Andreas F. Molisch[1,3]
[1]Dept. of Electroscience, Lund University, Box 118, SE-221 00 Lund, Sweden{E-mail: Firstname.Lastname@es.lth.se}
[2]Vienna University of Technology, Austria{E-mail:nicolai.czink@nt.tuwien.ac.at}
[3]Mitsubishi Electric Research Labs, 201 Broadway, Cambridge, MA 02139, USA

***Abstract*— In this paper, we present a cluster based analysis of an outdoor-to-indoor Multiple-Input Multiple-Output (MIMO) measurement campaign, and extract model parameters for the COST273 channel model. The measurements were performed at 5.2 GHz for 159 measurement locations in an office building. Multipath component (MPC) parameters have been extracted for these positions using a high-resolution algorithm. We analyze the clustering of MPCs, i.e., grouping together of MPCs with similar DOAs, DODs, and delays. We compare cluster identification by visual inspection to automatic identification by the recently proposed algorithm of Czink et al. In the paper we include results on the intercluster properties such as the distribution of the number of clusters and the cluster powers, as well as intracluster properties such as the angle and delay spreads within the clusters. In particular, we extract parameters for the COST 273 channel model, a standardized generic model for MIMO propagation channels.**

***Index Terms*— MIMO, Clustering multipath channel, COST273 channel model, Angle-spread, Delay-spread.**

I. Introduction

Multiple antennas at both receiver and transmitter can result in tremendous capacity improvements compared to single antenna systems. Ultimately, the capacity gains depend on the propagation channel in which the system is operating. The establishment of good channel models is therefore essential both for the development of new algorithms for signal processing, modulation and coding, and for the unified testing of different system proposals. A number of standardized channel models have been developed for the testing of specific systems, e.g., the 3GPP model for outdoor cellular communications [1] and the 802.11n model for indoor wireless LANs [2]. However, those models do not cover some important scenarios, especially the case where the base station is outdoors, and the mobile station is indoors. In recent conference contributions [3] [4], we presented measurement results for the outdoor-to-indoor case and presented some typical parameters like total rms angular spread. In the current paper, we use those measurements to derive a subset of the COST 273 model parameters that can be implemented for system testing.

In measured MIMO propagation channels the MPCs tend to occur in clusters, i.e., groups of MPCs with similar parameters, delay, direction of arrival (DOA), and direction of departure (DOD) [5], [6]. It is important that channel models correctly reflect this clustering property [7]. For example, the results in [8], indicate that channel models disregarding clustering effects overestimate capacity. Furthermore, from an aspect of system-level testing, it is convenient to model the propagation channel in terms of cluster properties rather than modeling the behavior of individual MPCs. It is for these reasons that clustering in MIMO propagation channels is actively researched, e.g., [6] [9] [10], and also included in many channel models. In particular, the European COST 273 [11] action has developed a general MIMO channel model that describes parameters for the MPC clusters occurring in the propagation channel. This description can be broadly categorized as *intercluster* and *intracluster* parameters which characterize the clusters and MPCs within clusters, respectively. The model is general enough to allow description of many different scenarios, e.g., cellular, WLAN, fixed wireless, and peer-to-peer communications.

In this paper we establish a set of parameters, for the clustered stochastic MIMO channel model for the outdoor-to-indoor case. The parameters are based on the COST 273 generic channel model and fitted with the results from our measurements. Though the COST 273 model is applicable both to time-variant and static channels, in this paper we characterize a static environment only. For that goal, we first perform a cluster identification; using both visual inspection and an automatic clustering algorithm [12]. In the remainder of the paper we include detailed results on the intercluster and intracluster properties, including cluster power distributions, and intracluster delay spreads and angular spreads.

II. Measurement setup

The measurement setup is described in detail in [3] and summarized here for the convenience of the reader. Measurement data were recorded with the RUSK ATM channel sounder. The measurements were performed at a center frequency of 5.2 GHz and a signal bandwidth of 120 MHz. The transmit antenna was an 8 element dual polarized uniform linear patch array and the receive antenna was a 16-element uniform circular array with vertically polarized monopole elements. The channel was seen to be static and this was confirmed by the measurements.

We have extracted MPC parameters for the 159 measurement positions using the high-resolution RIMAX algorithm [13]. At each measurement position we have extracted the parameters delay, DOA, DOD, and complex path-weights for up to 50 MPCs. It must be stressed that high-resolution algorithms based on the sum-of-plane-waves model cannot explain all possible

propagation processes, especially not in the indoor environment where the receive antenna sometimes was located close to some scatterers. However, the RIMAX algorithm estimates the parameters for the diffuse scattering component of the measured channel. The path parameters, DOA, DOD, and delay were cross-checked at a number of positions with the geometry of the measurement site, and provided a good match.

III. Comparison of Clustering Approaches

Clustering of MPCs, i.e., identification of MPCs that have similar parameters, is conventionally performed by visual inspection, e.g., [10], [14], [15]. To utilize the large data set from our 159 measurement locations, we have performed clustering with an automated algorithm proposed in [12]. For selected measurement locations, we also performed a *visual cluster identification* by a *joint-inspection* of parameter extraction results. The delay, DOA azimuth and DOD azimuth domains were jointly employed for clustering in both methods. Note that our cluster analysis is based on plane waves only and disregards the diffuse contributions.

For the visual inspection, a cluster was *identified* as a set of MPCs with similar delay, DOA, and DOD parameters - note that we require that all of the parameters must be similar in order for the MPCs to form a cluster. We also investigated the physical propagation mechanisms of the MPCs (e.g., reflections via specific objects), and required that MPCs belonging to a cluster should have the same physical propagation mechanisms. To avoid a bias by the observer, the clustering by visual inspection was performed $before$ automated clustering results were available. For the automated cluster identification, which was performed for all measurement locations, we *defined* clusters based on a power-weighted "multipath component distance" metric as defined in [12], [16]. Since powers of the extracted MPCs exhibit a large dynamic range, we limited our analysis to MPCs with powers within 30 dB of the strongest component. The weaker components have negligible influence on the calculation of statistical spreads but would introduce inaccuracies when calculating probability density functions such as for the number of clusters and number of MPCs per cluster.

The clustering for one measurement location is compared in Fig. 1 (visual) and Fig. 2 (algorithm). The clusters defined by the algorithm appear in reasonable agreement with the visually identified clusters. The algorithm defines three separate clusters for the MPCs otherwise identified as cluster 1 by visual inspection, similarly cluster 4 from visual identification is defined as two adjacent clusters. To compare the two clustering approaches, for all locations where visual inspection was performed, the respective CDFs for the intracluster spreads for delay, DOA and DOD are plotted in Figs. 3, 4, and 5. Note that for comparing the two clustering methods only a statistical measure, a CDF of the spreads, is employed because our final objective is to characterize the channel with statistical parameters rather than describe physical propagation. Based on the CDFs of the intracluster spreads, the two clustering approaches are in good agreement. The results in the remainder of the paper are based on automated clustering only.

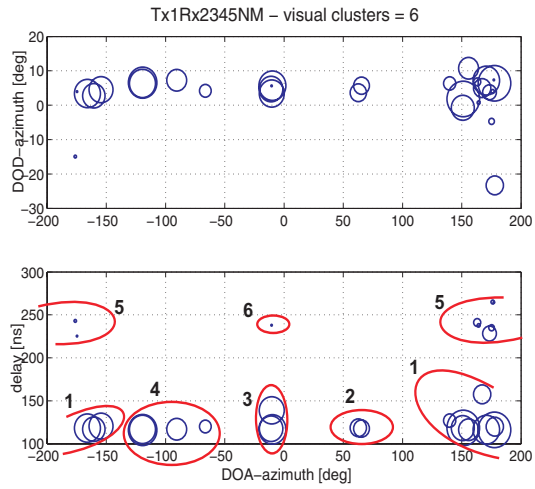

Fig. 1. Clusters identified by visual inspection at location Tx1Rx2345NM [3]. Circle diameters are scaled to relative powers of MPCs. Clusters 1 and 5 represent energy coming through the door, which opens into the office corridor. Clusters 4 (West wall) and 2 (East wall) represent reflections from metal objects on wall-racks. Clusters 3 and 6 are due to reflections from metal pipes of heater/ window handles along South wall. Clusters 5 and 6 are delayed from their earlier arriving counterparts, due to multiple reflection between the two buildings where Tx and Rx are placed.

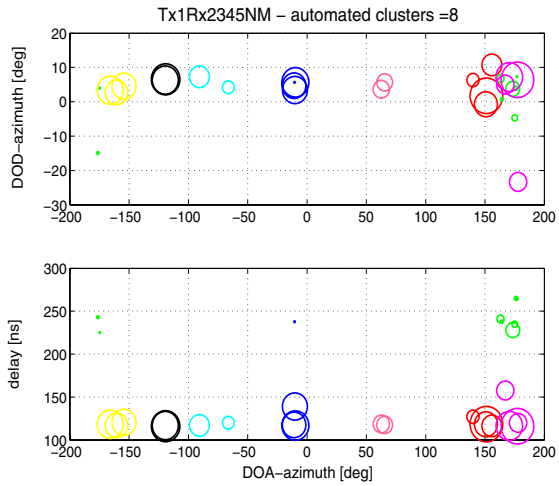

Fig. 2. Clusters defined by the algorithm at location Tx1Rx2345NM. The MPCs are color coded to indicate cluster association.

IV. Results

The clustering algorithm[1] was applied to all 159 measurement locations and a total of 1005 clusters were extracted. These form the statistical ensemble for the statistical analysis reported in this section. The results have been categorized as intra- and intercluster properties.

[1]A delay-scaling factor of 5 was used to assign more significance to delay during clustering. The Cluster-pruning feature of the algorith was not used owing to the upper limit of 50 MPCs extracted per position by RIMAX and a further 30 dB power limit on MPCs to be considered for cluster analysis.

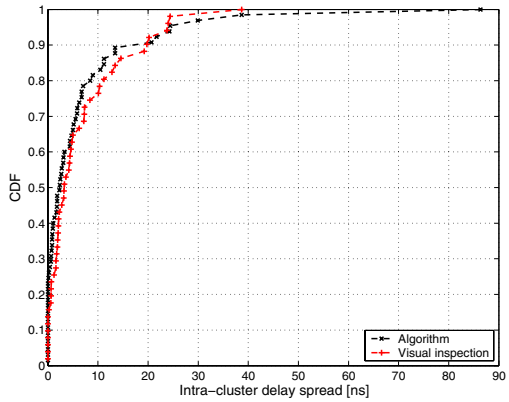

Fig. 3. Algorithm vs. visual inspection, comparison of CDFs of intra-cluster delay spread.

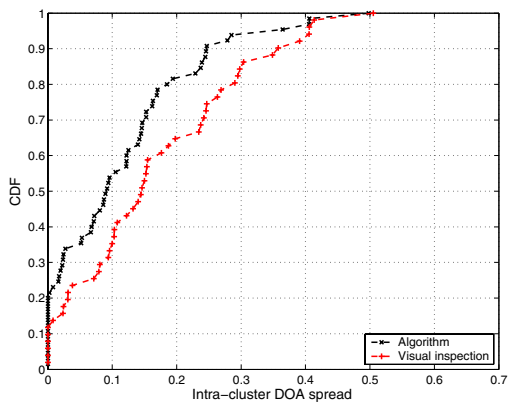

Fig. 4. Algorithm vs. visual inspection, comparison of CDFs of intra-cluster DOA spread.

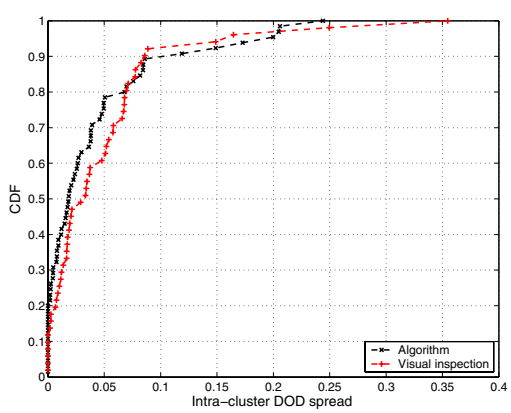

Fig. 5. Algorithm vs. visual inspection, comparison of CDFs of intra-cluster DOD spread.

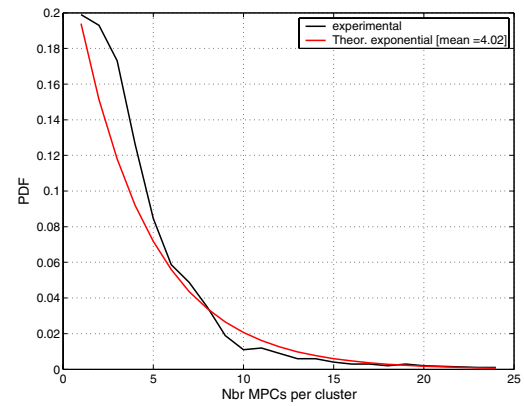

Fig. 6. Distribution of number of MPCs in a cluster.

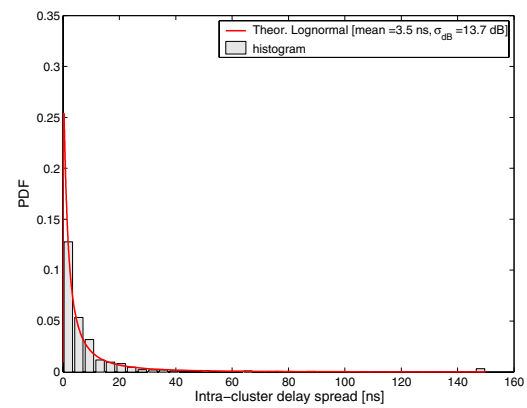

Fig. 7. Distribution of delay spread within a cluster.

A. *Intra-cluster properties*

The distribution of the number of MPCs per cluster is plotted in Fig. 6. The median number of MPCs is 3 whereas the mean is 4.02. An Exponential distribution with the indicated mean provides a good fit to the empirical pdf. The distribution of the intracluster delay spread is plotted in Fig. 7. The spread[2] is calculated as the conventional rms delay spread [5], of MPCs within a cluster. Note that the apparently large occurence of spreads around 150 ns is due to the fact that isolated occurences of the delay spread, in excess of 150 ns, have been collected into this single bin. According to the COST 273 model, a Lognormal pdf has been fitted to all intracluster spreads. For the delay spread, a mean of 3.5 ns and standard deviation of 13.7 dB provides a reasonable fit to the histogram.

The distribution of the spreads in direction of arrival and departure, azimuth only, are plotted in Figs. 8 and 9. To avoid the ambiguity caused by the origin of the coordinate system, the

[2]The delay spread model of COST 273 is distance-dependent, i.e., the delay spread is the product of $d^{-0.5}$ times the lognormal variable, where d is the Tx-Rx distance. However, we omit this scaling in our analysis because the distance variation in our measurements, between nearest and farthest Rx location relative to Tx, never exceeds a factor of 2.

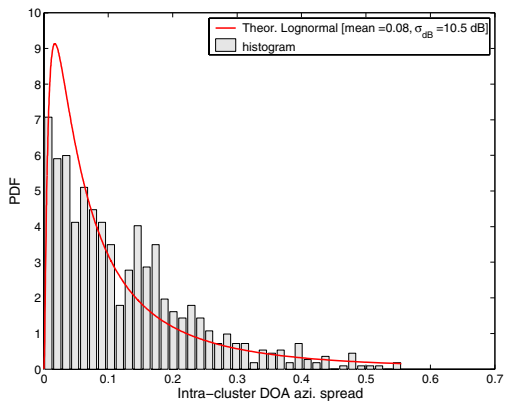

Fig. 8. Distribution of the DOA spread within a cluster.

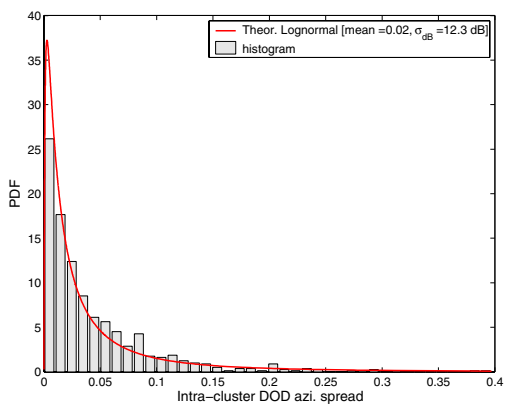

Fig. 9. Distribution of DOD spread within a cluster.

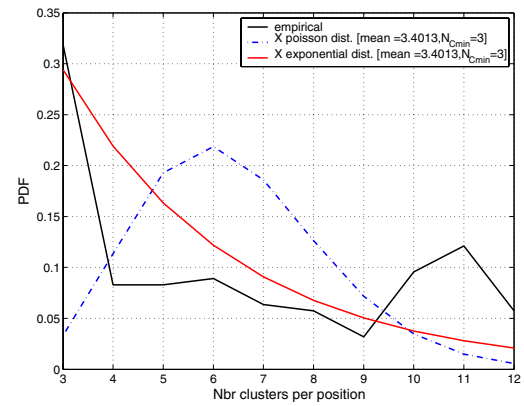

Fig. 10. Distribution of the number of clusters.

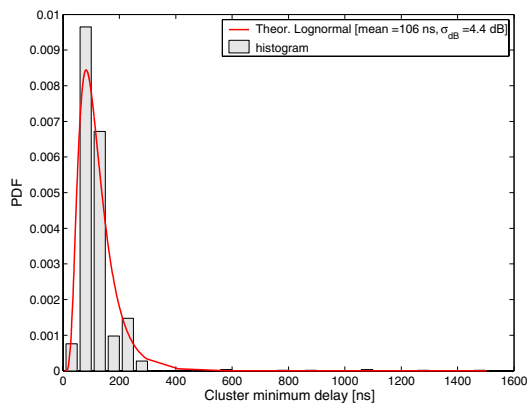

Fig. 11. Distribution of the minimum delay of the clusters.

Fleury definition [17] is used to calculate the spreads[3]. Note that in Figs. 7, 8, and 9 the singletone[4] clusters, which by definition have zero spread, are not plotted. A total of 200 out of the 1005 clusters were observed to be singletone clusters. For the DOA spread, a Lognormal pdf with mean 0.08 and deviation 10.5 dB has been fitted to the empirical PDF. For the DOD spread, a Lognormal with a mean of 0.02 and deviation of 12.3 dB fits our empirical results.

B. Inter-cluster properties

The distribution of the number of clusters at each measurement location is plotted in Fig. 10. The horizontal axis begins at 3 since at each measurement location, this is the lower limit of the range of possible number of clusters from which the algorithm selects the optimum cluster set. According to the COST 273 model, the total number of clusters is $N_{C_{\min}} + X$, where $N_{C_{\min}}$ is the minimum number of clusters occuring at each position (3 in our case) and X is a random variable with Poisson distribution. Though, this functional relation does not describe our measurements well, and choosing X as Exponential distributed seems to fit better. The mean number of clusters was found to be 6.4 while the median value was 6. The distribution of the minimum delays of the clusters, i.e., first-arriving component of each cluster is plotted in Fig. 11. The occurence of minimum delay values in excess of 400 ns is due to singletone clusters ocurring at this delay. A Lognormal distribution with mean 106 ns and deviation 4.4 dB was found to fit the empirical data. Due to space constraints in the paper, we omit our results on the distributions of the mean angle of arrival and departure. These results, together with the correlations between the cluster spreads and the cluster powers, will be discussed in a follow-up publication. In Fig. 12 the normalized cluster powers are plotted as a function of the excess minimum delays of the clusters, i.e., cluster delays relative to minimum delay of the first arriving cluster at the respective measurement location. The cluster powers are normalized by the power of the same cluster. Thus we are able to compare clusters from different measurement locations. The solid line in Fig. 12 is the linear regression of the cluster powers in dB on the

[3]The Fleury definition of direction spread can, for small values, be used as the angular spread in units of radians.

[4]Clusters consisting of a single MPC

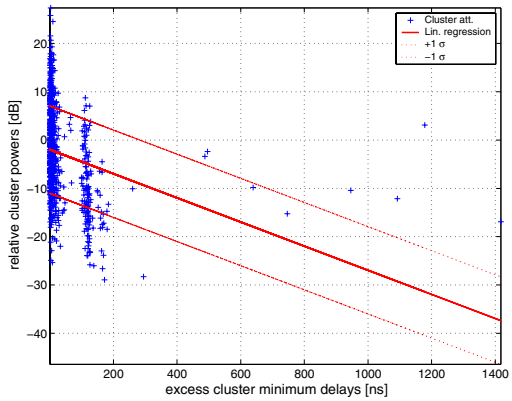

Fig. 12. Attenuation of cluster powers as a function of excess delay.

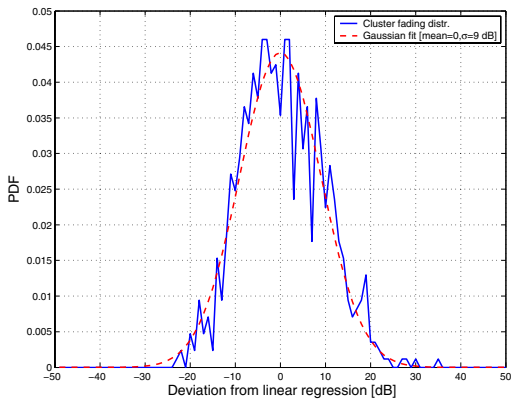

Fig. 13. Distribution of cluster shadow fading, and a zero-mean Gaussian fit.

excess minimum delays of the clusters, and indicates addittional attenuation depending on excess delays of the clusters. An attenuation coefficient of 25 dB/μs is observed from this plot. Note that we do not use a cut-off delay in plotting Fig. 12 because we have some late arriving clusters with strong powers. The deviation of the cluster powers from the linear regression is a measure of the cluster power shadow fading. In Fig. 13 an empirical PDF of the deviation is plotted together with a Gaussian fit with zero-mean and standard deviation of 9 dB. In Figs. 12 and 13 the first arriving clusters at each location, which have been used for normalization, are not plotted; these clusters would have coordinates $(0, 0)$ in Fig. 12 and would appear as a large peak around 0 in Fig. 13.

V. Summary

We have performed a statistical analysis of MPC clusters observed in our measurements at 159 locations in an outdoor-to-indoor office scenario. We extracted a subset of the model parameters of the COST273 channel model, valid for this scenario. For the intracluster properties, the number of MPCs per cluster was observed to be Exponentially distributed, the intra-cluster spreads followed a Lognormal distribution. For the intercluster properties, the distribution of number of clusters was better fit by an Exponential rather than the Poisson distribution specified in the model. The cluster delay was observed to follow a Lognormal distribution. The cluster attenuation coefficient was measured to be 25 dB/μs.

VI. Acknowledgement

We would like to thank Markus Landmann for useful inputs and TU Ilmenau for providing the antennas used in measurements. Part of this work was financed by an INGVAR grant of the Swedish Foundation for Strategic Research and a grant from the Swedish Science Council. This work was partly conducted within the EC-funded Network-of-Excellence NEWCOM.

References

[1] 3GPP - 3GPP2 Spatial Channel Model Ad-hoc Group, "Spatial channel model for MIMO systems," tech. rep., 3GPP and 3GPP2; download at http://www.3gpp.org, 2003.

[2] A. K. Jagannatham and V. Erceg, "MIMO indoor WLAN channel measurements and parameter modeling at 5.25 GHz," in *Proc. VTC 2004 Fall*, vol. 1, pp. 106–110, IEEE, September 2004.

[3] S. Wyne, P. Almers, G. Eriksson, J. Karedal, F. Tufvesson, and A. F. Molisch, "Outdoor to indoor office MIMO measurements at 5.2 GHz," in *VTC 2004 - Fall*, (Los Angeles, USA), pp. 101–105, September 2004.

[4] S. Wyne, A. F. Molisch, P. Almers, G. Eriksson, J. Karedal, and F. Tufvesson, "Statistical evaluation of outdoor-to-indoor office MIMO measurements at 5.2 GHz," in *VTC 2005 - Spring*, (Stockholm, Sweden), pp. 146–150, May/ June 2005.

[5] A. Saleh and R. A. Valenzuela, "A statistical model for indoor multipath propagation," *IEEE J. Selected Areas Comm.*, vol. 5, pp. 128–137, February 1987.

[6] J. Fuhl, A. F. Molisch, and E. Bonek, "Unified channel model for mobile radio systems with smart antennas," in *Proc. IEE Radar, Sonar and Navigation*, vol. 145, pp. 32–41, IEE, February 1998.

[7] A. F. Molisch, "Effect of far scatterer clusters in MIMO outdoor channel models," in *VTC 2003 - Spring*, (South Korea), pp. 534–538, April 2003.

[8] K. Li, M. Ingram, and A. V. Nguyen, "Impact of clustering in statistical indoor propagation models on link capacity," *IEEE Transactions on Communications*, vol. 50, pp. 521–523, April 2002.

[9] M. Steinbauer and A. F. Molisch(eds.), "Directional channel models," in *Wireless Flexible Personalized Communications* (L. Correia, ed.), ch. 3.2, pp. 132–193, Wiley, 2001.

[10] L. Vuokko, P. Vainikainen, and J. Takada, "Clusters extracted from measured propagation channels in macrocellular environments," *IEEE Transactions on Antennas and Propagation*, vol. 53, pp. 4089–4098, December 2005.

[11] L. Correia, ed., *COST 273 final report: Towards mobile broadband multimedia networks*. Elsevier, 2006. to appear.

[12] N. Czink, P. Cera, J. Salo, E. Bonek, J. Ylitalo, and J.-P. Nuutinen, "A framework for automatic clustering of parametric MIMO channel data including path powers," in *VTC 2006 - Fall*, (Montreal, Canada), September 2006.

[13] A. Richter, *Estimation of Radio Channel Parameters: Models and Algorithms*. PhD thesis, Ilmenau Technical University, Germany, 2005.

[14] N. Czink, X. Yin, E. Bonek, and B. Fleury, "Cluster angular spreads in a MIMO indoor propagation environment," in *PIMRC'05*, (Berlin, Germany), 2005.

[15] M. Toeltsch, J. Laurila, K. Kalliola, A. F. Molisch, P. Vainikainen, and E. Bonek, "Statistical characterization of urban spatial radio channels," *IEEE Journal on Selected Areas in Communications*, vol. 20, pp. 539–549, April 2002.

[16] M. Steinbauer, H. Özcelik, H. Hofstetter, C. F. Mecklenbräuker, and E. Bonek, "How to quantify multipath separation," *IEICE Trans. Electron.*, vol. 85, pp. 552–557, March 2002.

[17] B. H. Fleury, "First- and second-order characterization of direction dispersion and space selectivity in the radio channel," *IEEE Transactions on Information Theory*, vol. 46, pp. 2027–2044, September 2000.